

Near-Threshold η Meson Production in Proton–Proton Collisions

J. Smyrski¹, P. Wüstner², J.T. Balewski^{3,4}, A. Budzanowski³, H. Dombrowski⁶,
D. Grzonka⁵, L. Jarczyk¹, M. Jochmann², A. Khoukaz⁶, K. Kilian⁵, P. Kowina^{5,7},
M. Köhler², T. Lister⁶, P. Moskal¹, W. Oelert⁵, C. Quentmeier⁶, R. Santo⁶, G. Schepers^{5,6},
U. Seddik⁸, T. Sefzick⁵, S. Sewerin⁵, A. Strzałkowski¹, M. Wolke⁵

¹ *Institute of Physics, Jagellonian University, PL-30-059 Cracow, Poland*

² *ZEL, Forschungszentrum Jülich, D-52425 Jülich, Germany*

³ *Institute of Nuclear Physics, PL-31-342 Cracow, Poland*

⁴ *IUCF, Bloomington, Indiana, IN 47405, USA*

⁵ *IKP, Forschungszentrum Jülich, D-52425 Jülich, Germany*

⁶ *IKP, Westfälische Wilhelms–Universität, D-48149 Münster, Germany*

⁷ *Institute of Physics, Silesian University, PL-40-007 Katowice, Poland*

⁸ *NRC, Atomic Energy Authority, 13759 Cairo, Egypt*

(August 21, 2017)

Abstract

The production of η mesons has been measured in the proton-proton interaction close to the reaction threshold using the COSY-11 internal facility at the cooler synchrotron COSY. Total cross sections were determined for eight different excess energies (ϵ) in the range from $\epsilon = 0.5$ MeV to $\epsilon = 5.4$ MeV. The energy dependence of the total cross section is well described by the available phase-space volume weighted by FSI factors for the proton–proton and proton– η pairs.

PACS: 13.60.Le, 13.75.-n, 13.85.Lg, 25.40.-h, 29.20.Dh

Typeset using REVTeX

I. INTRODUCTION

Over the last few years, creation of mesons near threshold in the elementary nucleon–nucleon collision has become an important field for studies of meson production mechanisms as well as of meson–nucleon interactions. Measurements at the new generation of medium energy proton accelerators, storage rings with phase-space cooling of the beam as the IUCF–ring, CELSIUS and COSY, delivered high precision values of cross sections for the production of various mesons in the mass region up to 1 GeV/c². The experimental information gained so far is consistent with approximately constant production matrix elements when the final state interaction (FSI) is factored out. The pion production cross sections are described very precisely including only the proton–proton FSI, since the pion–proton interaction is comparatively weak close to threshold. Contrary, in the η meson production in proton–proton collisions the η –proton FSI can essentially influence the energy dependence of the total cross section. Effects of η –proton FSI have been seen in Dalitz plots from investigations at CELSIUS [1]. Inclusive measurements at CELSIUS [2] indicate additional contributions from partial waves of higher order than s–wave even at an excess energy as low as 36 MeV, which again change the energy dependence of the cross section according to their relative strength.

II. EXPERIMENT

Existing data on the $pp \rightarrow pp\eta$ reaction near threshold, originating from measurements at SATURNE using the spectrometers SPES–3 [3] and PINOT [4] and at CELSIUS [1] with the PROMICE/WASA detection system, still leave enough freedom for interpreting the energy dependence of the cross sections.

Therefore, further data of the pp induced η production very close to threshold were needed. Measurements were performed at the COoler SYnchrotron COSY [5] in Jülich with the use of the COSY–11 facility, shown schematically in Fig. 1, in the range of excess energies below $\epsilon = 6$ MeV.

The COSY-11 facility, described in detail in Ref. [6], uses an internal hydrogen cluster target [7], installed in front of a COSY accelerator dipole magnet. Due to their lower momenta, the two outgoing protons of the reaction $pp \rightarrow pp\eta$ are separated from the beam in the magnetic field of the C-shaped dipole and are diverted towards the direction of the centre of the synchrotron into the COSY-11 detector arrangement. Their trajectories are measured by means of hits in a set of two drift chambers (marked D1 and D2 in Fig. 1), allowing the momentum to be determined by ray tracing back through the precisely known magnetic field to the target position. Identification of particles (here protons) is performed by additionally measuring the time-of-flight over a distance of ≈ 9.4 m between start and stop scintillator hodoscopes (S1 and S3). The uncharged η mesons are not registered exclusively but are identified using the missing mass method.

Measurements were performed with the beam momentum varied continuously in the range from 9.6 MeV/c below to 20.4 MeV/c above the threshold momentum which is equal to 1981.6 MeV/c. For the data analysis, this range was grouped into 2 MeV/c intervals. In the following, the central momenta for these intervals and not their limits are quoted.

For different excess energies examples of missing mass distributions are shown in Fig. 2, each of them being dominated by a clear peak due to the η meson production, except for the case where the beam momentum is below the reaction threshold. The η missing mass distribution broadens with increasing excess energy, which is a kinematical effect. The square of the missing mass (MM) is determined by the square of the four-momentum vector evaluated when subtracting the sum of the two exit proton four momentum vectors ($\mathbf{P}_1 + \mathbf{P}_2$) from the one of the proton-proton entrance channel (\mathbf{P}_0):

$$MM^2 = (\mathbf{P}_0 - (\mathbf{P}_1 + \mathbf{P}_2))^2. \quad (1)$$

For the limit of $\epsilon \ll m_\eta$ it can be shown [8] that the resolution of the square of the missing mass is proportional to the experimental momentum resolution of the two protons measured (which is supposed to be constant for all excess energies in the range discussed here) times

$\sqrt{\epsilon}$:

$$\Delta(MM^2) = a \cdot \sqrt{\epsilon}. \quad (2)$$

Fitting the width distribution ($\Delta(MM^2)$) of the η missing mass peak as function of the excess energy in the present experiment at proton beam momenta around 2.0 GeV/c, as shown in Fig. 3, a value of $a_\eta = (390 \pm 20) \sqrt{MeV^3}/c^4$ was extracted.

III. DATA EVALUATION

The number of events corresponding to the η meson production was derived from the missing mass spectra. The background underneath the η peak, being due to the production of two to four pions, was determined using measurements below threshold. For this reason, a smoothed background measured below threshold has been shifted according to the kinematical limit of the missing mass spectra, shown as a dotted line in Fig. 2, and was scaled according to the ratio of luminosities for the beam momenta above and below threshold. The background is that low (peak to background ratio $\geq 40/1$) that the approximation of the smoothed background shown by the dashed line in Fig. 2 can hardly be seen.

Due to the rapid variation of near-threshold cross sections as function of beam momentum, a high precision knowledge of the absolute value of the beam momentum is extremely crucial for the present measurements. The present "nominal" beam momenta in the range around 2 GeV/c, calculated from the synchrotron frequency and the beam orbit length, are known at COSY with an accuracy of $\frac{\Delta p}{p} = 10^{-3}$ [5]. The corresponding uncertainty of the total cross section amounts to values as large as $\frac{\Delta\sigma_{TOT}}{\sigma_{TOT}} \approx \pm 50\%$ at $\epsilon = 2$ MeV.

When evaluating the missing mass spectra with the nominal COSY beam momenta the average of the η meson missing mass is shifted by about $+0.66$ MeV/c² compared to the η meson mass known from literature [9], as indicated in Fig. 2 by an arrow. This

discrepancy might partly be due to a systematic uncertainty in the detection system as incorrect assumptions of the magnetic fringe field or of the positions of the drift chambers ($\leq |0.28 \text{ MeV}/c^2|$) [10]. However, the corresponding correction of the beam momentum of $\Delta p = (-1.88 \pm 0.80) \text{ MeV}/c$ is in accordance with the $\frac{\Delta p}{p} = 10^{-3}$ uncertainty of the nominal beam momentum.

The relative uncertainty of the corrected beam momentum of $\delta p/p = 0.4 \cdot 10^{-3}$ is by a factor of two and a half smaller than the uncertainty of the beam momentum determined from the beam orbit length and the frequency of the synchrotron.

In the experiment proton–proton elastic scattering was measured simultaneously. The luminosity was determined by comparing differential counting rates with data obtained by the EDDA collaboration [11].

IV. DETERMINATION OF THE EXCESS ENERGY

Above, the best value for the true beam momenta at the eight different momentum intervals was determined by shifting the extracted η meson mass to its value known from the literature [9].

In the following we present a second method for a determination of the beam momenta, where the measured dependence of the $pp \rightarrow pp\eta$ counting rate on the beam momentum can be used to evaluate the beam momentum with high precision. The applied method is analogous to the one used by the COSY-11 collaboration for the beam energy determination in measurements of the $pp \rightarrow pK^+\Lambda$ reaction [12] and is largely independent of systematical uncertainties due to the magnetic fringe field or drift chamber positions. However, it assumes a phase space dependence modified by final state interactions of the total cross section close to threshold. The measured yield of the $pp \rightarrow pp\eta$ events (N) normalized to the integrated luminosity (L) is extrapolated as a function of the excess energy towards zero.

The corresponding offset of the excess energy was used to correct the nominal value of the excess energy:

$$N/L = C \cdot A(\varepsilon - \Delta\varepsilon) \cdot \sigma(\varepsilon - \Delta\varepsilon), \quad (3)$$

where C is a normalization factor, A is the acceptance of the detection system, σ is the total cross section and $\Delta\varepsilon$ is the searched correction of the nominal excess energy. The values of C and $\Delta\varepsilon$ are adjusted by the fitting procedure. The efficiency A is calculated using Monte Carlo simulations of the experiment assuming a uniform phase-space distribution of reaction products modified by the pp FSI. The influence of the ηp FSI on the acceptance is negligible.

The geometrical acceptance of the COSY-11 detection system is limited especially in the vertical direction due to the narrow opening of the dipole gap. The calculated efficiency includes also the inefficiency of detecting two close tracks due to limited double track resolution in the drift chambers equal to 3 mm.

The overall efficiency decreases from 31 % to 4.4 % in the range between the lowest and the highest excess energy measured. The energy dependence of the total cross section σ was assumed to be determined by the phase-space volume weighted by the proton–proton FSI factor, which was calculated as the squared absolute value of the complex amplitude of the proton–proton scattering amplitude in the effective range approximation with included Coulomb barrier penetration factor [13].

As shown in Fig. 4, the experimental data are well described by the applied function. The obtained correction to the excess energy is $\Delta\varepsilon = (-0.66 \pm 0.27)$ MeV, which means that the real excess energy is by that value smaller than the nominal one. The indicated error contains contributions due to final statistics of the data (± 0.06 MeV), due to the uncertainty of the detector acceptance (± 0.09 MeV), and due to the uncertainty of the mass of the η meson (547.30 ± 0.12) MeV/ c^2 [9], which influences the present result via the threshold energy. The correction coincides with the value found from the shift of the missing mass peak, the latter, as a model–free measure of the true excess energy, is used in the following.

V. TOTAL CROSS SECTIONS

The values of the total cross sections are given in Table I and are depicted in Fig. 5. The indicated vertical error bars denote the statistical uncertainty only. The overall systematic error amounts to 15 %, where 10 % originate from the determination of the detection efficiency and 5 % from the luminosity determination. Data from measurements at SATURNE with the spectrometers SPES-3 [3] and PINOT [4] and at CELSIUS [1] using the PROMICE/WASA system are added in Fig. 5 to the present results. The data are consistent and determine rather precisely the excitation function in the full range of the considered excess energies up to 40 MeV.

In order to describe the shape of the energy dependence of the cross sections one can assume that it is dominated by the available phase-space weighted by the $pp\eta$ FSI factor. The $pp\eta$ FSI can be factorized into pp (f_{pp}) and $p\eta$ ($f_{p\eta}$) factors and integrated over the available phase-space volume ρ_3 :

$$\sigma(\varepsilon) \sim \int f_{pp}(q_{pp}) \cdot f_{p\eta}(q_{p_1\eta}) \cdot f_{p\eta}(q_{p_2\eta}) d\rho_3, \quad (4)$$

where q_{pp} is the relative momentum of two protons and $q_{p_1\eta}$ and $q_{p_2\eta}$ are the relative momenta of the η meson with respect to first and second proton, respectively. The enhancement factors for the η -proton FSI were calculated in the effective range approximation with the complex η -proton scattering length $a_{\eta p} = 0.717 + i0.263$ taken from Ref. [14] and the complex η -proton effective range parameter $r_{\eta p} = -1.50 - i0.24$ from Ref. [15]. The calculations shown by the solid line in Fig. 5 describe the experimental data in the whole range of excess energy. Omission of the η -proton FSI leads to discrepancies with the data as shown by the dashed curve. At the same time, a calculation neglecting the proton-proton Coulomb interaction (dotted curve) fails to reproduce the energy dependence of the data within the limits of the relative uncertainty in the true beam energy.

VI. CONCLUSIONS

The total cross section of the reaction $pp \rightarrow pp\eta$ was measured close to the kinematical threshold. The present results together with other available data determine the energy dependence of the cross section in a wide excess energy range above threshold. This dependence is well reproduced by the phase-space integral, weighted by the full $pp\eta$ final-state interaction. In particular, inclusion of the η -proton FSI as well as the proton-proton Coulomb interaction is essential for the description of the data.

Acknowledgements

We appreciate the work provided by the COSY operating team and thank them for the good cooperation and for delivering the excellent proton beam. The research project was supported by the BMBF (06MS881I), the Polish Committee for Scientific Research (2P03B-047-13), and the Bilateral Cooperation between Germany and Poland represented by the Internationales Büro DLR for the BMBF (PL-N-108-95). The collaboration partners from the Westfälische Wilhelms-University of Münster and the Jagellonian University of Cracow appreciate the support provided by the FFE-grant (41266606 and 41266654, respectively) from the Forschungszentrum Jülich. One of the authors (P.M.) acknowledges the hospitality and financial support from the Forschungszentrum Jülich and the Foundation for Polish Science.

REFERENCES

- [1] H. Calén et al., Phys. Lett. **B 366** (1996) 39.
- [2] H. Calén et al., Phys. Lett. **B 458** (1999) 190.
- [3] A. Boudard, Few-Body Systems Suppl. **8** (1995) 287,
F. Hibou et al., Phys. Lett. **B 438** (1998) 41.
- [4] E. Chiavassa et al., Phys. Lett. **B 322** (1994) 270.
- [5] R. Maier, Nucl. Instr. & Meth. **A 390** (1997) 1.
- [6] S. Brauksiepe et al., Nucl. Instr. & Meth. **A 376** (1996) 397.
- [7] H. Dombrowski et al., Nucl. Instr. & Meth. **A 386** (1997) 228.
- [8] J. Smyrski for the COSY-11 collaboration, Annual Report 1999, to be reported in:
Berichte des Forschungszentrums Jülich, (2000).
- [9] Review of Particle Physics, Eur. Phys. J. **C 3** (1998) 25.
- [10] P. Moskal et al., Annual Report 1997, Berichte des Forschungszentrums Jülich, Jül-3505
(1998) 41.
- [11] D. Albers et al., Phys. Rev. Lett. **78** (1997) 1652.
- [12] J. Balewski et al., Phys. Lett. **B 420** (1998) 211.
- [13] B. J. Morton et al., Phys. Rev. **169** (1968) 825.
- [14] T. -S. H. Lee, Physica Scripta **58** (1998) 15.
- [15] A. M. Green and S. Wycech, Phys. Rev. **C 55** (1997) R2167.

TABLES

TABLE I. Total cross sections for the $pp \rightarrow pp\eta$ reaction

Beam momentum (GeV/c)	Excess energy (MeV)	Total cross section (μb)
1.98315	0.54	0.022 ± 0.004
1.98515	1.24	0.121 ± 0.012
1.98715	1.94	0.27 ± 0.02
1.98915	2.64	0.37 ± 0.03
1.99115	3.34	0.49 ± 0.04
1.99315	4.04	0.70 ± 0.05
1.99515	4.73	0.68 ± 0.06
1.99715	5.43	0.89 ± 0.07

The uncertainties of the beam momenta and the excess energies are:
 ± 0.00080 GeV/c and ± 0.28 MeV, respectively.

The listed errors of the total cross sections include statistical uncertainties only,
the additional systematic error amounts to $\pm 15\%$.

FIGURES

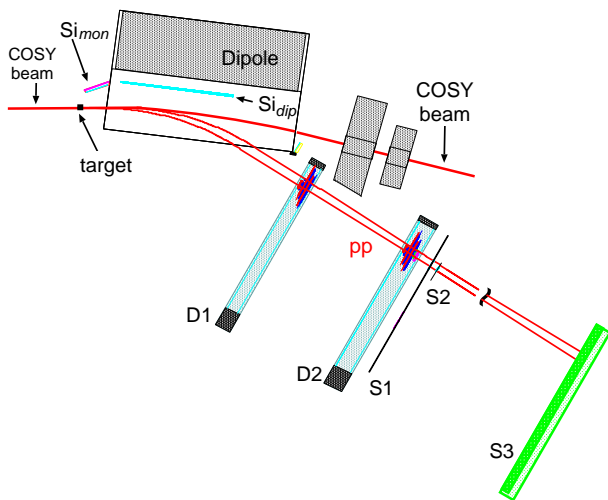


FIG. 1. Schematic view of the COSY-11 facility. The particle trajectories are measured by means of hits in two sets of drift chambers D1 and D2. The scintillation hodoscopes S1 and S2 are used as start detectors and S3 as the corresponding stop detector for time of flight measurements.

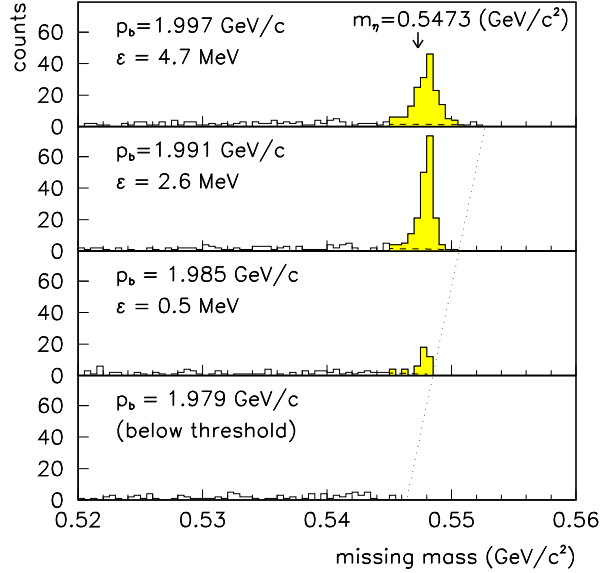


FIG. 2. Missing mass spectra with respect to the proton–proton system measured for three different momenta above and one momentum below threshold. The dotted line indicates the kinematical limit of the missing mass distribution. The dashed line underneath the η peaks represents the background determined from measurements below threshold.

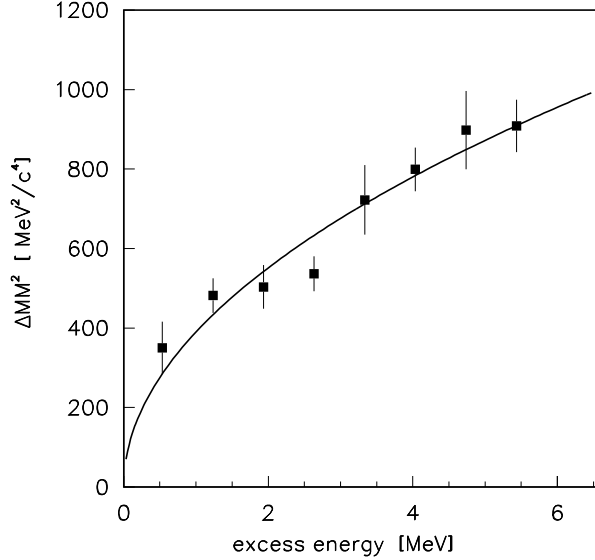


FIG. 3. Width of the η missing mass peak as a function of the excess energy. Experimental data points represent the width extracted from the central momenta of the momentum bins applied, the solid line corresponds to a fit using eq. (2) with the parameter $a_\eta = 390 \sqrt{MeV^3}/c^4$.

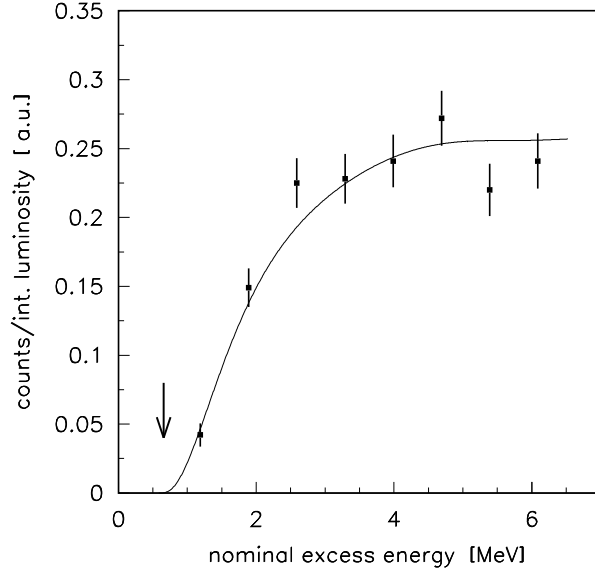


FIG. 4. Determination of the absolute value of the beam momentum by extrapolating the $pp \rightarrow pp\eta$ counting rate towards the threshold. The curve is given by eq. 3, the fit results in $\chi^2 = 1.5$ per degree of freedom. The arrow corresponds to the resulting correction of the excess energy of $\varepsilon = (-0.66 \pm 0.27)$ MeV.

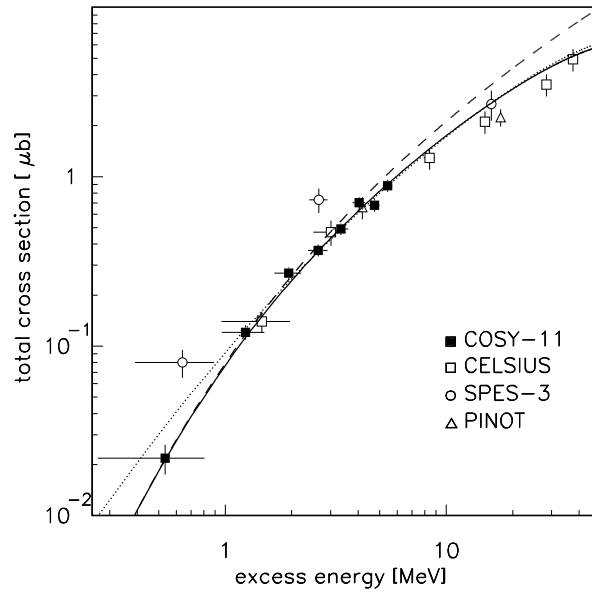


FIG. 5. Total cross sections for the reaction $pp \rightarrow pp\eta$ near threshold.

Vertical error bars denote the statistical errors and the horizontal error bars show the systematical error of 0.28 MeV. The relative excess energy uncertainty is 0.01 MeV (see Ref. 12), i.e. below the size of the symbols.

Solid line: Phase-space distribution weighted by the proton–proton FSI
and Coulomb interaction plus proton– η FSI,

Dashed line: omission of proton– η FSI from the solid line,

Dotted line: omission of proton–proton Coulomb interaction from the solid line.